USGS
science for a changing world

Prepared for the National Aeronautics and Space Administration

Geologic Map of the Mylitta Fluctus Quadrangle (V–61), Venus

By Mikhail A. Ivanov and James W. Head, III

Pamphlet to accompany
Scientifiic Investigations Map 2920

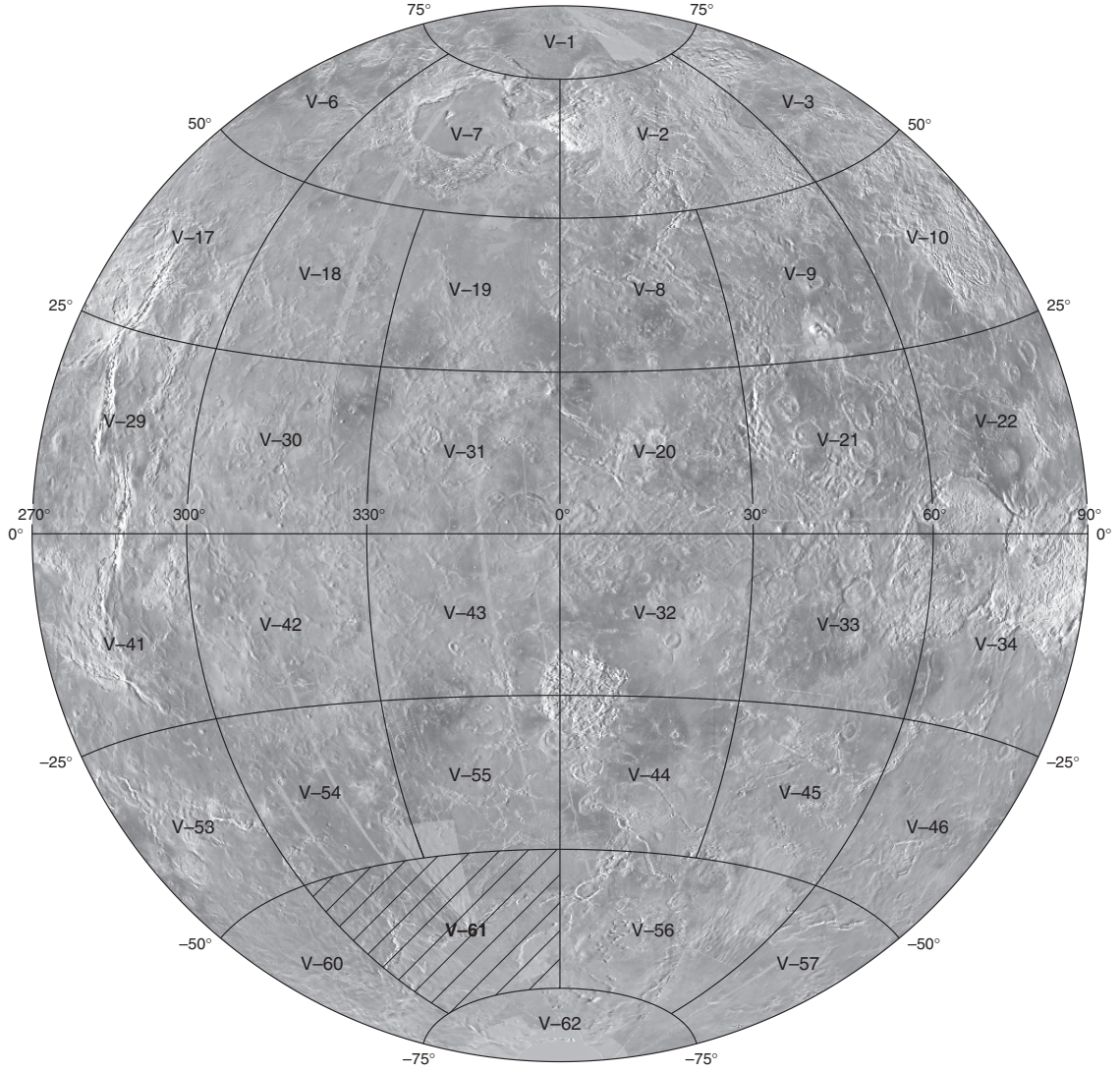

2006

U.S. Department of the Interior
U.S. Geological Survey

INTRODUCTION

THE MAGELLAN MISSION

The Magellan spacecraft orbited Venus from August 10, 1990, until it plunged into the Venusian atmosphere on October 12, 1994. Magellan Mission objectives included: (1) improving knowledge of the geological processes, surface properties, and geologic history of Venus by analysis of surface radar characteristics, topography, and morphology, and (2) improving the knowledge of the geophysics of Venus by analysis of Venusian gravity.

The Magellan spacecraft carried a 12.6-cm radar system to map the surface of Venus. The transmitter and receiver systems were used to collect three data sets: (1) synthetic aperture radar (SAR) images of the surface, (2) passive microwave thermal emission observations, and (3) measurements of the backscattered power at small angles of incidence, which were processed to yield altimetric data. Radar imaging, altimetric, and radiometric mapping of the Venusian surface was done in mission cycles 1, 2, and 3 from September 1990 until September 1992. Ninety-eight percent of the surface was mapped with radar resolution on the order of 120 meters. The SAR observations were projected to a 75-m nominal horizontal resolution, and these full-resolution data compose the image base used in geologic mapping. The primary polarization mode was horizontal-transmit, horizontal-receive (HH), but additional data for selected areas were collected for the vertical polarization sense. Incidence angles varied between about 20° and 45°.

High resolution Doppler tracking of the spacecraft took place from September 1992 through October 1994 (mission cycles 4, 5, 6). Approximately 950 orbits of high-resolution gravity observations were obtained between September 1992 and May 1993 while Magellan was in an elliptical orbit with a periapsis near 175 km and an apoapsis near 8,000 km. An additional 1,500 orbits were obtained following orbit-circularization in mid-1993. These data exist as a 75° by 75° harmonic field.

MAGELLAN RADAR DATA

Radar backscatter power is determined by (1) the morphology of the surface at a broad range of scales and (2) the intrinsic reflectivity, or dielectric constant, of the material. Topography at scales of several meters and larger can produce quasi-specular echoes and the strength of the return is greatest when the local surface is perpendicular to the incident beam. This type of scattering is most important at very small angles of incidence because natural surfaces generally have few large tilted facets at high angles. The exception is in areas of steep slopes, such as ridges or rift zones, where favorably tilted terrain can produce very bright signatures in the radar image. For most other areas, diffuse echoes from roughness at scales comparable to the radar wavelength are responsible for variations in the SAR return. In either case, the echo strength is also modulated by the reflectivity of the surface material. The density of the upper few wavelengths of the surface can have a significant effect. Low-density layers, such as crater ejecta or volcanic ash, can absorb the incident energy and produce a lower observed echo. On Venus, there also exists a rapid increase in reflectivity at a certain critical elevation, above which high-dielectric minerals or coatings are thought to be present. This leads to very bright SAR echoes from virtually all areas above that critical elevation.

The measurements of passive thermal emission from Venus, though of much lower spatial resolution than the SAR data, are more sensitive to changes in the dielectric constant of the surface than to roughness. As such, they can be used to augment studies of the surface and to discriminate between roughness and reflectivity effects. Observations of the near-nadir backscatter power, collected using a separate smaller antenna on the spacecraft, were modeled using the Hagfors expression for echoes from gently undulating surfaces to yield estimates of planetary radius, Fresnel reflectivity, and root-mean-square (rms) slope. The topographic data produced by this technique have horizontal footprint sizes of about 10 km near periapsis, and a vertical resolution on the order of 100 m. The Fresnel reflectivity data provide a comparison to the emissivity maps, and the rms slope parameter is an indicator of the surface tilts, which contribute to the quasi-specular scattering component.

MYLITTA FLUCTUS QUADRANGLE

The Mylitta Fluctus quadrangle (V–61, fig. 1) is in the southern hemisphere of Venus and extends from lat 50° to 75° S. and from long 300° to 360° E. The northern third of the quadrangle covers the southern part of Lavinia Planitia, which represents a class of equidimensional lowlands on Venus (Bindschadler and others, 1992b) and is as deep as about 1.5–2 km below mean planetary radius. The southeastern part of the map area shows the western part of the upland of Lada Terra, the summit of which is about 3 km above mean planetary radius (fig. 2).

Before the Magellan mission, the geology of the Mylitta Fluctus quadrangle was known on the basis of topographic data acquired by the Pioneer-Venus altimeter (Masursky and others, 1980; Pettengill and others, 1980) and radar images received by the Arecibo telescope (Campbell and others, 1991). Arecibo radar images showed that the area of Mylitta Fluctus quadrangle was populated by several coronae and coronalike features and riftlike fracture zones parallel to the northern margin of the upland of Lada Terra (Campbell and others, 1991; Senske and others, 1991). Arecibo data further revealed that the western and southern parts of the map area were characterized by complex patterns of features such as deformational belts and volcanic plains. Several regions along the margins of Lada Terra upland were thought to be the sources of extensive outpourings of digitate lava flows down the regional slopes of Lada.

Early Magellan results showed that the interior of Lavinia Planitia was populated with complex patterns of deformational features in the form of belts of ridges and grooves (Squyres and others, 1992; Solomon and others, 1992). The most prominent belts of ridges within the map area are Molpadia and Penardun Lineas at the southern edge of Lavinia Planitia and Morrigan Linea west of Lada Terra. The upland of Lada Terra

hosts an assemblage of numerous coronae including one of the largest corona on Venus, Quetzalpetlatl (Stofan and others, 1992), interconnected by belts of fractures and graben (Baer and others, 1994; Magee and Head, 1995). One of these belts, Kalaipahoa Linea, runs from east to west through the middle of the Mylitta Fluctus quadrangle connecting Kamui-Huci Corona in the west-central part and Jord Corona and Tarbell Patera in the eastern part of the map area. Among the most spectacular features of the quadrangle are large complexes of lava flows, Mylitta Fluctus (Roberts and others, 1992) emanating from Tarbell Patera and Cavillaca Fluctus and Juturna Fluctus originating at Boala Corona, which is inside larger Quetzalpetlatl Corona. Magellan gravity data (Konopliv and Sjogren, 1994; Konopliv and others, 1999) show that the eastern half of the quadrangle, which is dominated by the western part of Lada Terra, is characterized by high values of both vertical gravity acceleration (as much as 120 mGal) and height of geoid (as much as 40 m). Lowlands that surround the upland are characterized by a –30 mGal gravity anomaly and a –10 m geoid anomaly northwest and southwest of the Lada Terra upland.

The key geological theme of the quadrangle is that the map area portrays a transition zone from uplands to lowlands. The characteristics and configuration of Lavinia Planitia north of the map area have been cited as evidence for the region being the site of large-scale mantle downwelling (Bindschadler and others, 1992b). The topographic configuration, gravity signature, and pattern of deformation belts in Lada Terra are consistent with mantle upwelling under the upland (Kiefer and Hager, 1991). Thus, the region of Mylitta Fluctus quadrangle represents a laboratory for the study of the formation and evolution of lowlands and highlands, the emplacement of volcanic plains, the formation of associated tectonic features, and their relation to mantle processes. The major questions addressed by geological mapping in the Mylitta Fluctus quadrangle include the following: What is the sequence of events in the formation and evolution of large-scale lowlands and uplands on Venus? What are the characteristics of the marginal areas surrounding these topographic provinces? When did the transition zone from Lada Terra to the lowlands form? How do the units in Mylitta Fluctus quadrangle compare with each other and what information do they provide concerning models for Venus global stratigraphy and tectonic history? These issues and questions are the basis for our geologic mapping analysis.

In our analysis we have focused on the geologic mapping of the Mylitta Fluctus quadrangle using traditional methods of geologic unit definition and characterization for the Earth (for example, North American Commission on Stratigraphic Nomenclature, 1983) and planets (for example, Wilhelms, 1990) appropriately modified for radar data (Tanaka, 1994). We defined units and mapped key relations using the full-resolution Magellan synthetic aperture radar (SAR) data (mosaicked full-resolution basic image data records, C1-MIDR's, F-MIDR's, and F-Maps) and transferred these results to the base map compiled at a scale of 1:5 million. In addition to the SAR image data, we incorporated into our analyses digital versions of Magellan altimetry, emissivity, Fresnel reflectivity, and roughness data (root mean square, rms, slope). The background for our unit definition and characterization is described in Tanaka (1994), Basilevsky and Head (1995a, b), Basilevsky and others (1997), and Ivanov and Head (1998).

MAGELLAN SAR AND RELATED DATA

The synthetic aperture radar (SAR) instrument flown on the Magellan spacecraft (12.6 cm, S-band) provided the image data used in this mapping and interpretation. SAR images are a record of the echo (radar energy returned to the antenna), which is influenced by surface composition, slope, and wavelength-scale surface roughness. Viewing and illumination geometry also influence the appearance of surface features in SAR images. Guidelines for geologic mapping using Magellan SAR images and detailed background to aid in their interpretation can be found in Elachi (1987), Saunders and others (1992), Ford and Pettengill (1992), Tyler and others (1992), and Tanaka (1994). In the area of the Atalanta Planitia quadrangle, incidence angles are such, 16.3–21.3 for Cycle 1 and 19.7–25.1 for Cycle 2 (Ford and others, 1993), that backscatter is dominated by variations in surface roughness at wavelength scales. Rough surfaces appear relatively bright, whereas smooth surfaces appear relatively dark. Variations also occur depending on the orientation of features relative to the incident radiation (illumination direction), with features normal to the illumination direction being more prominent than those oriented parallel to it. Full-resolution images have a pixel size of 75 m; C1-MIDR's contain the SAR data displayed at ~225 m/pixel. Altimetry data and stereo images were of extreme importance in establishing geologic and stratigraphic relations between units. Also essential in the analysis of the geology of the surface are data obtained by Magellan on the emissivity (passive thermal radiation), reflectivity (surface electrical properties), and rms slope (distribution of radar wavelength scale slopes). Aspects of these measurements were used in unit characterization and interpretation; background on the characteristics of these data and their interpretation can be found in Saunders and others (1992), Ford and Pettengill (1992), Tyler and others (1992), Tanaka (1994), and Campbell (1995).

GENERAL GEOLOGY

Several geologic processes have influenced the Mylitta Fluctus quadrangle and have combined to form its geologic record. Volcanism is apparently the dominant process of crustal formation on Venus (Head and others, 1992) and produced most of the observed geologic units in the map area. These units typically have a plainlike appearance. There are two meanings of the term "plains" (Mescherikov, 1968). In a strict morphological sense, plains define morphologically uniform surfaces with relatively small differences in relief. In a broader sense, plains are counterparts of highlands and define vast flat terrains. In the strict sense, the term "plains" is simply a descriptor of a type of the surface and does not bear an interpretative meaning. At the higher level of interpretation is the term "volcanic plains" that implies knowledge or inference of

the nature of material that makes up the plains. In the case of Venus, the materials that form plains are most likely volcanic. In the broader sense the term "plains" usually describes large physiographic provinces (for example, North American Plain, Russian Plain). Thus, the same term can be applied to define two different classes of morphologic and (or) physiographic features. Although the specific meaning of term "plains" is usually clear from the context, misunderstanding in the usage of it may occur. Fortunately, in planetary nomenclature the physiographic and physiographic-topographic meanings of the term "plains" are strictly defined. A vast plainlike and mainly homogeneous physiographic province is called "planitia" if it is at mid- to low elevations (for example, Atalanta Planitia or Isidis Planitia) or "planum" if it is elevated (for example, Lakshmi Planum or Hesperia Planum). Following this rule, we use the term "plains" in the nongenetic, morphological sense throughout the map text and description of map units. On the basis of their specific morphologic and physical property characteristics, we define various plains units. For example, lobate plains differ from shield plains.

The volcanic and volcano-tectonic features that occur within the quadrangle and are related to the larger and more distinct sources are listed in table 1. Tectonic activity has modified some of these basic crustal materials (for example, Solomon and others, 1992; Squyres and others, 1992) in a variety of modes (extension and contraction). In places deformation is so extensive, as in the case of ridge belts, that the deformational features become part of the definition of the material unit (see also Tanaka, 1994; Scott and Tanaka, 1986). Impact cratering (table 2) has also locally influenced regions in the quadrangle but has not been an influential process over the map area as a whole. Aeolian processes require a source of sediment to produce deposits and such deposits are therefore concentrated around impact craters (for instance, crater Meitner) and localized around tectonic fractures and scarps (for example, Greeley and others, 1992).

In places, clusters of small shield volcanoes less than about 15 km in diameter (Aubele and Slyuta, 1990; Guest and others, 1992; Aubele, 1994, 1995; Crumpler and Aubele, 2000; Addington, 2001) are common in spatial association with deformation belts that complicate the surface within the lowlands surrounding Lada Terra. Individual small shields, however, occur relatively rarely within the vast extent of regional plains that cover the surface between the belts and within most of Lada Terra. The small shields are low in elevation, commonly have a summit pit, do not appear to have distinct associated flows, and are commonly embayed by subsequent regional plains deposits (for example, Kreslavsky and Head, 1999; Ivanov and Head, 2001b). Concentrations of small shield volcanoes occur predominantly in the western part of the quadrangle. A cluster of steep-sided domes (Pavri and others, 1992) has been found in the northwest corner of the Mylitta Fluctus quadrangle.

Coronae are common features within the quadrangle. They are concentrated mostly within the upland of Lada Terra while the territory of Lavinia Planitia lacks coronae (Stofan and others, 1992, 2001; Crumpler and others, 1993; Crumpler and Aubele, 2000; Ivanov and Head, 2001a). Distinct complexes of lava flows (fluctuses) are in close spatial association with coronae situated within Lada Terra. For instance, Jord Corona and Tarbell Patera nearby represent the source region for Mylitta Fluctus; Boala Corona, which is completely inside Quetzalpetlatl Corona, is the source of Cavillaca and Juturna Fluctuses. In contrast, Kamui-Huci Corona, which has no associated distinct lava flows, is at the level of the lowlands surrounding Lada Terra. Distinct flowlike features that compose fluctuses clearly indicate both the source regions and flow paths. The flows of the most distinct fluctuses follow the present-day topography meaning that the relief in the areas of the flows did not change significantly since their emplacement. The most prominent volcanic and volcano-tectonic features within the Mylitta Fluctus quadrangle (Crumpler and Aubele, 2000) are listed in table 1.

Approximately the western half of the quadrangle consists of plains with relatively homogeneous radar brightness interpreted to be of volcanic origin, and modified by tectonic structures to varying, but usually low, degrees. These plains are mostly concentrated within the lowlands surrounding Lada Terra upland and their source vents are not known. Some of these plains display radar backscatter variations and apparent flow fronts that permit stratigraphic distinctions among subunits. A significant area in the eastern half of the quadrangle is covered by plains and flowlike features, also interpreted to be of volcanic origin, that are characterized by radar brightness varying from low to high. The plains and flowlike features are almost tectonically undeformed and typically associated with distinct sources such as coronae. The composition of the homogeneous and inhomogeneous volcanic plains is not known from data in this quadrangle although Venera 9, 10, 13, and 14 (northeastern and southeastern slope of Beta Regio) and Vega 1 and 2 (Ursula Planitia) lander geochemical analyses of sites in similar terrains suggest compositions similar to terrestrial basalts (Basilevsky and others, 1992).

The area of the Mylitta Fluctus quadrangle lacks occurrences of tessera where several tectonic styles have operated together or in sequence to produce terrain more heavily deformed than typical regional plains and where the deformation is so intense that it becomes a major part of the unit definition (for example, Bindschadler and others, 1992a). Tectonic features in the Mylitta Fluctus quadrangle (fig. 3) are mostly present in several deformation belts that consist of either contractional or extensional structures. In some places, however, extensional structures complicate deformational belts that predominantly consist of contractional ridges. In the northeastern part of the quadrangle the southern ends of two large deformation belts, Penardun Linea and Molpadia Linea, are visible and another belt, Morrigan Linea, runs in a north-northeast direction in the western part of the map area. These belts, which are about 100 to 150 km wide, are among the most prominent structures on the floor of the lowlands surrounding Lada Terra and represent dense swarms of ridges, which are typically 5 to 10 km wide. Within the upland of Lada Terra, ridge belts are less prominent and occur on the northern regional slope of the upland, and an arc of a belt of ridges forms the western and northern parts of the rim of Quetzalpetlatl Corona. Wrinkle

ridges are widespread throughout the regional plains that cover most of the surface of the lowlands around Lada Terra and occur as windows among the inhomogeneous plains and lava flows within the upland. The typical length of wrinkle ridges is several tens of kilometers and width is a few kilometers. Wrinkle ridges and ridge belts manifest contractional deformation.

The northern edge of the Lada Terra upland (fig. 2) is outlined by a large belt of extensional structures (fractures and graben), Kalaipahoa Linea (figs. 1, 3), that runs for about 2,200 km in an easterly direction from Kamui-Huci Corona through Jord Corona and Tarbell Patera to the eastern margin of the quadrangle. The typical width of Kalaipahoa Linea is about 150-200 km. Extensional features in the quadrangle include individual narrow (less than about 1–2 km) graben hundreds of kilometers in length that apparently radiate away from the area of Jord Corona (figs. 1, 3).

Nine impact craters have been mapped in the quadrangle (fig. 4, table 2). The craters range in diameter from 9.3 km for crater Nadeyka to 149.0 km for crater Meitner (Herrick and others, 1997; Schaber and others, 1998, table 2). No splotches (surface markings and deposits interpreted to be formed from airblasts from projectiles traversing the atmosphere; for example, Schaber and others, 1992; Ivanov and others, 1992) were detected in the quadrangle. Although unambiguous surface deposits emplaced during the cratering event (both outflow deposits and dark haloes; Schaber and others, 1992; Phillips and others, 1992; Campbell and others, 1992; Schultz, 1992) have not been noted, occurrences of dark, featureless plains surround crater Meitner. This spatial association may suggest that the plains (at least in part) represent remnants of a dark halo. There are no areas within the quadrangle apparently covered with fragmental surface materials that have been redistributed by aeolian processes.

STRATIGRAPHY

On the basis of an analysis of the global size-frequency distribution of impact craters, a crater retention age of 800 Ma (McKinnon and others, 1997), 500 Ma (Schaber and others, 1992; Phillips and others, 1992) or 300 Ma (Strom and others, 1994), for the present surface of Venus has been proposed. The crater areal distribution cannot be distinguished from a spatially random population, which, together with the small total number of craters, means that crater size-frequency distributions cannot be used to date stratigraphic units for an area the size of the Mylitta Fluctus quadrangle (Hauck and others, 1998; Campbell, 1999). Therefore, attention must be focused on the definition of geologic units and structures, as well as analysis of crosscutting, embayment, and superposition relations among structures and units to establish the regional geologic history.

Although we have mapped tectonic structures independently of geologic units, in a few cases tectonic features are such a pervasive part of the morphology of the terrain that it becomes part of the definition of a unit. For example, our units of plains with wrinkle ridges are analogous to Member 1 of the Arcadia Formation on Mars ("Low-lying plains; mare-type (wrinkle) ridges common", Scott and Tanaka, 1986) and ridged plains material ("Characterized by broad planar surfaces ... and long parallel, linear to sinuous mare-type (wrinkle) ridges...", Scott and Tanaka, 1986; Greeley and Guest, 1987). In recently published Venus maps, the same approach of unit definition was successfully applied for mapping of several quadrangles that portray geologically diverse provinces (Rosenberg and McGill, 2001; Bridges and McGill, 2002; Campbell and Campbell, 2002; Hansen and DeShon, 2002). In other cases, the approach depends on scale and density of structures. For example, where the structures are more discrete and separated, we mapped them separately (fig. 3) and not as a specific unit. In other cases, where structures are very dense, tend to obscure the underlying terrain, and are embayed by younger material units, we chose to map such occurrences of pervasive tectonic structures as specific units. Here we summarize the stratigraphic units and structures and their relations.

Densely lineated plains material (unit pdl, figs. 5, 6). The stratigraphically oldest plains unit is densely lineated plains material (unit pdl), which is characterized by relatively flat surfaces on a regional scale and by swarms of parallel and subparallel lineaments (resolved as fractures if they are wide enough) having typical spacing of less than 1 km. Occurrences of the unit are typically small, 200–300 km long and as much as 100 km wide, and the total area of the plains is about 0.07 x 10^6 km^2 or about 0.9 percent of the area of the quadrangle (table 3). Although the unmodified precursor terrain for the densely lineated plains material is not observed, the flatness of the surface suggests that it was plains. The fractures that deform the surface of the unit are structural elements. However, they are such a pervasive part of the morphology of this terrain that it becomes a key aspect of the definition of the unit (see Campbell and Campbell, 2002; Hansen and DeShon, 2002 or several of the Mars examples cited above). Densely lineated plains occur predominantly in the northern half of the quadrangle, within the lowlands surrounding Lada Terra upland, often in close association with belts of ridges. Small patches of the plains are also visible northwest of Quetzalpetlatl Corona and inside it.

Ridged and grooved plains material (unit prg, figs. 5, 6, 7). Following the emplacement and deformation of densely lineated plains, a plains material with relatively high radar backscatter was emplaced. This unit, ridged and grooved plains material (unit prg), is commonly deformed by relatively broad (5–10 km wide) ridges tens of kilometers long. In the Mylitta Fluctus quadrangle this unit is arranged in linear outcrops or belts, Morrigan Linea, Penardun Linea, and Molpadia Linea (figs. 1, 3), 100 to 150 km wide and as much as 2,300 km long (Morrigan), and is largely equivalent to the ridge belts of Kryuchkov (1990), Frank and Head (1990), Squyres and others (1992) and to units mapped in the other quadrangles on Venus (Rosenberg and McGill, 2001; Bridges and McGill, 2002). Ridges are the dominant structures of the belts. Although the ridges are structural elements, they are important features that help to define and map the material unit of ridged and grooved plains. For instance, there is not much doubt that wrinkle ridges deform materials that form regional wrinkle-ridged plains. Hypotheti-

cally, a wrinkle ridge or collection of them would represent kipukas of material of unit pwr if younger lavas would flood the rest of the unit. If this hypothetical situation is mapped at a scale sufficient to outline individual exposures (wrinkle ridges) of a material largely covered by younger material then the true structural elements, wrinkle ridges, should be mapped as a material unit. The scale of our mapping is mostly sufficient to map exposures of a material unit represented on the surface by arches and ridge belts. This is unit prg and it is a material unit, although it is represented mostly by structures.

Occasionally, sparse grooves that are both subparallel and oblique to the strike of the ridges are seen. Although the grooves appear to cut the ridges, they are confined within the belts. The area occupied by ridged and grooved plains material is about 0.41 x 10^6 km^2 or about 5.4 percent of the quadrangle (table 3). Ridged and grooved plains are probably volcanic plains materials deformed into ridgelike belts by compression. The plains occur primarily in the western and northern parts of the quadrangle and some of them (Penardun and Molpadia) represent southernmost extension of the ridge belt concentration in the Lavinia Planitia area (north of the map area, Ivanov and Head, 2001a). Occurrences of ridged and grooved plains material are oriented predominantly north-northeast in the western and northern parts of the Mylitta Fluctus quadrangle (fig. 3), but at the southeastern edge of the quadrangle the ridge belts form the arcuate rim of Quetzalpetlatl Corona.

Shield plains material (unit psh, figs. 5, 7, 8). Following the emplacement and deformation of ridged and grooved plains material shield plains material (unit psh) of intermediate radar albedo was emplaced. This unit is characterized by abundant small shield-shaped features ranging from a few kilometers in diameter up to about 10–20 km, many of them with summit pits. Although small clusters of shields were recognized earlier planet wide (Head and others, 1992), they were considered localized occurrences possibly related to individual sources such as hot spots. Later work in Vellamo Planitia (Aubele, 1994, 1995) recognized that many of these occurrences represented a stratigraphic unit in this region, and subsequently this unit has been recognized in many areas on the planet (Basilevsky and Head, 1995b; Basilevsky and others, 1997; Crumpler and Aubele, 2000, Ivanov and Head, 1998, 2001a,b), including this quadrangle. Shields characterizing this unit occur in clusters, which give the unit a locally hilly texture, and as isolated outcrops in relatively smooth plains. The shields are probably volcanic in origin and are likely to be the sources of the adjacent smooth plains material. In the Mylitta Fluctus quadrangle, however, there is no clear evidence for specific flow units associated with the small edifices of shield plains. The unit is widely distributed in the quadrangle but occurs predominantly in its western part within the lowlands around Lada Terra upland. The area of the unit is about 0.64 x 10^6 km^2 or about 8.4 percent of the map area (table 3). Quite often, occurrences of shield plains material associate with the belts of ridges, Morrigan, Penardun, and Molpadia Linea. There are almost no concentrations of shield plains material in the central and eastern parts of the quadrangle (the Lada Terra upland), where the plains were either completely buried by younger plains units or never formed. Some isolated occurrences of shields occur where subsequent plains units embay shield plains and form kipukas (flooding the bases of the shields and leaving the tops exposed). Because the radar brightness of the two units commonly is different, we can estimate the thickness (about 100–200 m) of the margins of the embaying unit because we have information on the topography of the shields (Guest and others, 1992; Kreslavsky and Head, 1999).

Wrinkle ridged plains material (figs. 5, 8, 9). After the emplacement of these earlier plains units, the most widespread plains unit in the quadrangle, wrinkle-ridged plains material, was emplaced. The total area of the plains is about 3.88 x 10^6 km^2 or about 35.9 percent of the quadrangle. This unit is composed of morphologically smooth, homogeneous plains material of intermediate-dark to intermediate-bright radar albedo complicated by narrow linear to anastomosing wrinkle ridges (a structural element) in subparallel to parallel lines or intersecting networks. This unit is analogous to the ridged unit of the plateau sequence on Mars (Scott and Tanaka, 1986), which is a plains unit defined by "long, linear to sinuous mare-type (wrinkle) ridges." In the map area, the wrinkle ridges typically are less than 1 km wide and tens of kilometers long; in some areas they may be smaller, whereas in others they are larger. Although their trend often varies locally even within one site, the general orientation of the ridges is south-north (fig. 3). The unit is interpreted to be regional plains of volcanic origin that were subsequently deformed by wrinkle ridges, in some cases during the time of emplacement of the unit as a whole. Volcanic edifices and sources of the plains material are not obvious, although some small shield-shaped features are seen that appear to be kipukas of shield plains material (material unit psh).

On the basis of the typical pattern of the radar backscatter, wrinkle-ridged plains material is subdivided into two units. The lower unit (unit pwr_1, figs. 8, 9) generally has a homogeneous and relatively low radar albedo but can be mottled locally. This unit makes up the floor of the lowlands surrounding Lada Terra upland and occurs predominantly between elongated highs composed of preexisting units and ridge belts in the western and northern parts of the map area (for example, between Morrigan Linea and Penardun Linea in the west-central and northeastern parts of the quadrangle). The total area of the unit is about 2.08 x 10^6 km^2 or about 27.1 percent of the map area (table 3). The upper unit (unit pwr_2, fig. 9) appears to have slightly higher radar albedo and, in places, is characterized by lobate boundaries. The largest area of this unit occurs in the south-central part of the quadrangle that corresponds to the western regional slope of Lada Terra upland. Smaller occurrences of this unit are scattered within the quadrangle and are concentrated mostly at its northern and western edges. Totally, this unit makes up about 0.67 x 10^6 km^2 or 8.8 percent of the area of the quadrangle. Together these two units form about 36 percent of the surface of the quadrangle (table 3) and occur predominantly in low-lying regions surrounding Lada Terra upland.

The plains that are younger than regional plains are characterized by distinctive lobate and digitate shapes and margins,

morphologically smooth surfaces, and, in places, clusters of small shield-like features similar to those typical of the material unit of shield plains. The surface of these units is commonly unmodified by wrinkle ridges and other structural elements. Four types of the younger plains units are recognized.

Shield cluster material (unit sc, figs. 5, 10). The surface of this unit appears to be morphologically similar to that of shield plains (unit psh) but, in contrast, is tectonically undeformed and displays distinct small lava flows superimposed on lava plains nearby. The very small (100–150 km across) but distinct and mappable occurrences of this unit are within the deformation belt of Kalaipahoa Linea (inside and near Tarbell Patera, fig. 1) and occupy only about 0.003×10^6 km^2 or about 0.1 percent of the map area (table 3).

Smooth plains material (unit ps, figs. 5, 11). Smooth plains material is characterized by uniform and preferentially low albedo. Patches of this unit occur mostly in the western and northern parts of the quadrangle where some of them are in close spatial association with large impact crater Meitner (table 2). The total area of smooth plains is about 0.54×10^6 km^2 or about 7.1 percent of the map area (table 3).

A very significant part of the quadrangle (about 2.08×10^6 km^2 or 27.1 percent) is made up of lobate plains material, figs. 5, 9, 12) that has internal elements arranged in parallel to sinuous to lobate radar bright and dark strips and patches, and unit boundaries are typically lobate. On the basis of the typical pattern of lobate flow features and the characteristic relationship of superposition we have subdivided the material unit of lobate plains into two subunits. The lower unit of lobate plains (unit pl_1, figs. 5, 12) occupies a significant part of the northeastern quarter of the quadrangle and occurs on the northern and southern regional slopes of Kalaipahoa Linea. The total area of the unit is about 0.9×10^6 km^2 or 11.8 percent. This unit is characterized by a somewhat subdued pattern of lobate flows and both embays and is cut by fractures and graben composing the Linea. The upper unit of lobate plains (unit pl_2, figs. 5, 9, 12) is characterized by a very prominent pattern of lobate flows that embay most tectonic structures including those that deform the surface of the unit pl_1. There are two large areas where the upper unit of lobate plains occurs (both in eastern half of the quadrangle). The first is a huge complex of lava flows, Mylitta Fluctus, that occurs on the northern regional slope away from Lada Terra upland (fig. 4). The second is centered at Quetzalpetlatl and Boala Coronae the interiors of which and significant areas outside Quetzalpetlatl are covered by complexes of lava flows that have a specific lobate pattern. Boala Corona, which is completely inside Quetzalpetlatl, is the source of Cavillaca and Juturna Fluctuses that extend southwest of Quetzalpetlatl (fig. 4). The total area of the unit is about 1.18×10^6 km^2 or 15.4 percent.

Impact crater material (unit c, figs. 5, 13). Impact craters and related deposits are observed in several places in the quadrangle (fig. 4). Their locations are noted by symbols and they are mapped as undivided crater material (material unit c) of various diameters with proximal textured deposits. There are no impact craters within the mapped area that are characterized by distinct surrounding radar dark material (Campbell and others, 1992; Ivanov and others, 1992) that partly to mostly obscures the underlying terrain. In the quadrangle there is one crater (Alcott, 66 km in diameter, table 2) that is heavily embayed by lava flows of the upper unit of lobate plains material (unit pl_2) and there are no craters that are cut by tectonic features.

STRUCTURES

A variety of extensional and contractional tectonic structures is observed and mapped in the quadrangle (fig. 3).

Extensional structures. Long linear fractures and some paired and inward-facing scarps mapped as sharp grooves interpreted to be graben are seen in the northeastern quarter of the quadrangle. They are as much as 300–350 km long and appear to originate at Jord Corona. The graben and fractures produce a radiating pattern to the north of the corona (Nike Fossae) and to the south of Jord Corona the more uniformly oriented graben (in a south-southeast direction) form a swarm (Enyo Fossae) that runs from Jord Corona toward Quetzalpetlatl Corona. These structures clearly cut the surface of the lower unit of lobate plains material (unit pl_1) and are embayed by the upper unit of lobate plains material (unit pl_2).

In some cases, the extensional structures such as fractures and graben are so closely spaced that they tend to obscure underlying terrain and their presence takes on a defining character of the terrain. These concentrations are characterized by numerous short and long curvilinear subparallel lineaments that are usually wide enough to be resolved as fractures and graben. These occurrences form linear belts (groove belt unit gb, figs. 5, 14) a few hundreds of kilometers long and 50 to 60 km wide that are characterized by generally high topography compared to the surrounding plains. In detailed mapping at the F-Map scale, remnants of preexisting plains can be seen between the neighboring tectonic features. Orientations of grooves in the belts are generally parallel to the trend of the groove belts as a whole. Groove belts are concentrated in the west-central and northwestern parts of the quadrangle and a distinctive chain of groove belt occurrences extends from Kamui-Huci Corona in northwestern direction (fig. 3). Groove belts (unit gb) are distinguished from densely lineated plains material (unit pdl) by their belt-like form, a lower density of tectonic features, and the character of the fractures (more distinctly recognizable graben in unit gb). Groove belts also appear to be relatively distinct stratigraphically. The structures of the belts are mostly embayed by shield plains material (unit psh) and by wrinkle ridged plains material (units pwr_1 and pwr_2). Thus, these plains units represent the upper stratigraphic limit for the groove belts. The lower limit is, however, uncertain because fragments of the belts are not in direct contact with other units that are older than the vast regional plains material (units psh, pwr_1, and pwr_2).

Kalaipahoa Linea (figs. 1, 3) that runs in an east-northeast direction for about 2,200 km from the center of the quadrangle (Kamui-Huci Corona, table 1) to its eastern margin represents a dense set of relatively broad (up to a few kilometers wide) subparallel graben (figs. 5, 15). The structures of the Kalaipa-

hoa belt of graben complicate the summit of the broad and low topographic ridge outlining the northern edge of the Lada Terra upland and isolated, elongated, and equidimensional depressions occur along the central axis of the belt. These morphologic and topographic characteristics of Kalaipahoa Linea closely resemble those of rift zones elsewhere on Venus. The rift zone unit (unit rt) of Kalaipahoa Linea appears to be quite distinctive stratigraphically. Structures of the rift zone display evidence for simultaneous formation with the lower unit of lobate plains (material unit pl_1, fig. 15) but are clearly embayed by the upper unit of lobate plains material (unit pl_2, fig. 10).

Contractional structures. Several types and scales of contractional features are observed within the quadrangle (fig. 3). Wrinkle ridges are seen throughout the quadrangle and are so important in the broad regional plains that they in part define and characterize wrinkle-ridged plains material (fig. 9). These features are mapped in a representative sense in terms of density and trend by individual wrinkle ridge symbols. There is one predominant, south-north trend of the wrinkle ridges in the quadrangle. Wrinkle ridges are common structures within the western half of the map area where material units of shield plains and wrinkle ridged plains are the most important. In contrast, there are almost no wrinkle ridges in the eastern half of the quadrangle (fig. 3) where relatively young plains units (units ps, pl_1 and pl_2) dominate the area. Thus these units appear to form an upper stratigraphic limit for the wrinkle ridges development within the map area.

Ridged and grooved plains material (unit prg) is dominated by ridges and arches (figs. 6, 7, 15), and the general trends of these are also represented in the units by symbols. Ridged and grooved plains material forms predominantly north-northeast and northeast-trending bands or belts (fig. 3) that are largely equivalent to the ridge belts of Squyres and others (1992). Basilevsky and Head (1995a, b) described a structure (ridge belts, RB), which was a belt consisting of a cluster of densely spaced ridges 5–10 km wide and a few tens of kilometers long; this unit is often transitional to ridged and grooved plains material (unit prg). Although we did not map ridge belts in this area, the belts of ridged and grooved plains are closely related. For instance, a significant number of large occurrences of unit prg within Morrigan Linea and Penardun Linea represent typical ridge belts. The northern rim of Quetzalpetlatl Corona is morphologically also a ridge belt, although it is unclear whether it is a fragment of regionally developed ridge belts or a feature related to the evolution of the corona itself.

STRATIGRAPHIC RELATIONSHIPS OF UNITS

The material units and structures mapped commonly reveal relationships of superposition (embayment) and cross-cutting that either clearly display or strongly suggest relative ages among the units. Relationships between the oldest units in the map area, densely lineated plains and ridged and grooved plains material are shown in figure 6. Densely lineated plains material (unit pdl) occurs as an elongated area of irregular shape, the surface of which is dissected by densely packed short and narrow lineaments oriented west-northwest. Ridged and grooved plains (material unit prg) form an elongated topographic ridge (arch), oriented in a north-northeast direction, that is deformed by sparse narrow ridges and grooves that are roughly parallel to the arch strike. The occurrences of both units are broadly embayed by later plains units, implying that units pdl and prg make up the bottom of the stratigraphic column.

Although occurrences of densely lineated plains and ridged and grooved plains materials are not in direct contact, they are close to each other (the distance is less than 20 km, fig. 6) and are characterized by a very dissimilar structural pattern. Pervasive lineaments deforming the surface of unit pdl are completely absent within occurrences of unit prg, the surface of which is much less deformed by structures of different types. The difference in the character, density, and orientation of structures suggests that material of ridged and grooved plains was emplaced after both emplacement and deformation of material of densely lineated plains. In other localities, however, the relationships between these two units are less clear and densely lineated plains and ridged and grooved plains materials are shown significantly overlapping each other in the correlation chart.

Much more clear relationships, which are also consistent throughout the map area, are observed between ridged and grooved plains material and shield plains material (unit psh, fig. 7). In the area shown in figure 7 the material of ridged and grooved plains is deformed to different degrees and forms a belt of relatively narrow ridges. The ridges are approximately parallel to each other and oriented north-northeast. Material that surrounds occurrences of unit prg is only slightly deformed and characterized by abundant small shield features, commonly with summit pits (shield plains material, unit psh). Fragments of ridged and grooved plains appear as either heavily embayed relatively high standing contiguous massifs or as small elongated outliers of individual ridges. These relationships unambiguously mean that the shield plains material (unit psh) is younger and that the regional compressional stresses responsible for the deformation of ridged and grooved plains into ridge belts significantly waned by the time of emplacement of the shield plains.

Throughout the map area, consistent relationships of embayment occur between shield plains material (unit psh) and the lower unit of regional wrinkle-ridged plains material (unit pwr_1, fig. 8). In many areas within the quadrangle, the shield plains occur as tight clusters of small shieldlike structures, which is a characteristic feature of this unit elsewhere on Venus (Crumpler and Aubele, 2000; Addington, 2001). Clusters of shields form equidimensional fields tens of kilometers across surrounded by wrinkle ridged plains material as shown in figure 8. The clusters have slightly different radar albedo and typically are outlined by clear sinuous contacts that follow edges of individual shields at the boundaries of the clusters (see also Aubele, 1994). There is no evidence for flows emanating from any of the shields and superposed on the surface of surrounding regional plains. The density of shields is sharply diminished across the cluster boundaries and only a few small

isolated edifices are seen between neighboring clusters. These shields have no flows superposed on the surrounding plains.

These relationships between units of shield plains and regional wrinkle-ridged plains strongly suggest that the shields (clustered or individual) represent kipukas of a unit (shield plains material, unit psh) heavily flooded by younger regional wrinkle-ridged plains material (unit pwr_1). Indeed, Kreslavsky and Head (1999) have shown detailed quantitative examples of such relationships illustrating how isolated shields become smaller and less dense away from the contact, suggesting embayment by younger plains. Although these relative ages are typical within the map area, one cannot rule out the possibility of partly contemporaneous emplacement of shield plains and regional plains. To account for this uncertainty, these two units are shown partly overlapped in the correlation chart.

Both units of the regional wrinkle-ridged plains (lower unit, unit pwr_1, and upper unit, unit pwr_2) are deformed by a pervasive network of wrinkle ridges and, thus, predate the episode(s) of formation of the ridges (figs. 8, 9). The upper unit of wrinkle-ridged plains is typically brighter in SAR images and in places this unit is characterized by lobate boundaries resembling lava flows. These occurrences of the upper unit of wrinkle-ridged plains material apparently extend along local depressions and tend to outline local highs on the surface of the unit pwr1. This suggests that unit pwr_2 generally postdates, but may be locally correlative with, the lower unit of regional wrinkle-ridged plains material (unit pwr_1).

Consistent relationships between regional wrinkle-ridged plains and younger plains units (mostly lobate plains materials, units pl_1 and pl_2) are observed within the map area (figs. 9, 11). In each locality where these units are in contact the lobate and (or) smooth plains are almost tectonically undeformed and clearly embay structures of wrinkle ridges. This means that volcanic activity responsible for the formation of lobate plains began here after the formation of wrinkle ridges stopped. In places, there are clear relationships between two units of lobate plains material (units pl_1 and pl_2) that establish the relative ages between them (fig. 12). In the example shown in figure 12, the surface of the lower unit of lobate plains is cut by a system of long narrow graben that are partly to completely flooded by material of the upper unit of lobate plains. These relationships mean that here the unit pl_1 predates emplacement of the unit pl_2. A lava flow shown in the center of figure 12 is in close spatial association with one of the graben, and thus suggests that the graben was the source of the flow. In the lower right part of the image, another distinct lava flow (bright feature within unit pl_2) displays delta-like shapes oriented toward the ends of graben. These relationships of the graben (the southern end of the Enyo Fossae graben system, fig. 3) and the upper unit of lobate plains strongly suggest that the graben are the surface manifestation of dikes that propagated from the Jord Corona volcanic center. This interpretation is supported by the common presence of elongated rounded depressions (or pit chains) with associated lava flows at the other end of the graben near Jord Corona.

More complex relationships are observed between the upper units of lobate plains material and shield cluster material (units pl_2 and sc, fig. 10). Unit sc makes up a very small part of the map area (about 0.1 percent, table 3), but this unit is important in understanding the history of volcanism within the quadrangle. In the center of Jord Corona, a small cluster of shieldlike features occurs and these are morphologically similar to the shields characterizing the surface of shield plains material (unit psh) elsewhere in the map area. In contrast to the edifices of the unit psh, the shields of the unit sc are often seen as sources of distinct lava flows superimposed on the surface of surrounding lobate plains material (unit pl_2). The numerous shields nearby, however, appear as kipukas completely embayed by material of the unit pl_2 (fig. 10). These relationships of both embayment and superposition mean alternating emplacement of part of the units pl_2 and sc during about the same time interval. These relationships show that small shields are sometimes associated with large volcanic centers regardless of their ages. Although there is no reason to suspect that a specific small volcanic landform should be limited to a specific occurrence in time, our results in this quadrangle support our findings and those of others that small shields are abundant and form a specific unit (unit psh) lower in the stratigraphic column (Aubele, 1994, 1995; Ivanov and Head, 2001a,b; Bridges and McGill, 2002).

The only case of embayment of an impact crater (Alcott) within the map area is shown in figure 13. The crater is heavily flooded by the upper unit of lobate plains material (unit pl_2) that filled the crater interior through breaches in the northwest part of the rim. In the southeast part of the crater, the ejecta appear to be pristine and superimposed on the surface of the lower unit of lobate plains material (unit pl_1). Thus, the Alcott impact event apparently occurred between the episodes of emplacement of the two units of lobate plains.

Groove belts and ridges and arches that deform ridged and grooved plains material (unit prg) are rarely in contact. A number of observations collectively suggest that a groove belt, a fragment of which is shown in figure 14, predates surrounding regional plains: (1) a patchy areal distribution of short swarms of grooves that resemble fragments of more continuous zone; (2) abrupt termination of grooves at one end of short swarms and their collective reappearance in another swarm that continues the general trend; (3) the groove belt is cut by structures of wrinkle ridges; (4) association of the groove belt with a narrow zone of slightly elevated terrain. Where structures of the groove belt are in contact with ridges of unit prg there is clear evidence that the groove belt cuts through the ridges. Thus, the determination of the relative timing among units prg, gb, and pwr appears to be as follows: material of prg was emplaced and then deformed by broad ridges; these ridges were cut by structures of the groove belt and both gb and prg were embayed by regional plains material (pwr units), the material of which was finally deformed by pervasive narrow wrinkle ridges. These relationships imply a younger age of deformation within groove belts. The rare occurrences of interactions between the groove and ridge belts, however, introduce significant uncertainty in determination of their relative ages. Thus, they are shown overlapping in the correlation chart. The structures that form ridge and groove belts are embayed by regional

wrinkle-ridged plains material (unit pwr_1) meaning that both types of deformation occurred largely before emplacement and deformation of material of the regional plains.

The late extensional structures that form the deformational belt of Kalaipahoa Linea (interpreted as a rift zone) reveal both embayment and crosscutting relationships with the lower unit of lobate plains material (unit pl_1, fig. 15). Thus, the extensional deformation and emplacement of early lobate plains material were approximately contemporaneous. The structures of the rift zone, however, are heavily embayed by the upper unit of lobate plains material (unit pl_2) near Jord Corona. This relationship implies that the late major episodes of extension occurred mostly before formation of the youngest volcanic materials in the map area.

GEOLOGIC HISTORY

The area of Mylitta Fluctus quadrangle is a transitional zone from a large upland of Lada Terra to surrounding lowlands, one of which is Lavinia Planitia (figs. 1, 2), and, thus, is an important region for analysis of processes of lowlands and uplands formation and volcanic flooding. Major questions addressed by geologic mapping within the quadrangle are as follows: What is the sequence of events in the formation and evolution of large-scale lowlands and uplands on Venus? What are the characteristics of the marginal areas surrounding these topographic provinces? When did the transition zone from Lada Terra to the lowlands form? How do the units in Mylitta Fluctus quadrangle compare with each other and what information do they provide concerning models for Venus global stratigraphy and tectonic history? Here we discuss stratigraphic positions of units, their temporal correlation, and the implied geologic history of the region. We also examine the sequence of tectonic deformation and its interpretation as well as the evolution of volcanic and tectonic styles.

Mylitta Fluctus quadrangle lies within a vast tessera-free area in the southern hemisphere of Venus (Ivanov and Head, 1996). In this aspect, the quadrangle is in contrast to many other areas on Venus where tessera terrain typically forms the oldest material unit (Ivanov and Basilevsky, 1993; Ivanov and Head, 1996; Hansen and others, 1997; Phillips and Hansen, 1998). This specific feature of the map area means that either tessera never formed there or it was completely covered by subsequent lava plains units. Typically, tessera occurrences have much more significant relief compared with the occurrences of densely lineated plains material (unit pdl) (Ivanov and Head, 2001b). Thus, being embayed by later volcanic plains material, tessera occurrences have more chance to remain exposed. The presence of small fragments of unit pdl scattered throughout the map area and the absence of tessera fragments suggest that tessera terrain did not form within the area of Mylitta Fluctus quadrangle; these observations favor the hypothesis of a true global asymmetry of tessera distribution (Ivanov and Head, 1996). It should be noted that a large fragment of tessera terrain, Cocomama Tessera, characterizes the central part of Lada Terra (V–56, Lada Terra quadrangle). However, Cocomama Tessera is the only significant tessera massif within a latitudinal zone from 50° to 75° S. corresponding to the northern and southern margins of the map area.

Volcanic plains material that has been densely fractured (unit pdl) is the stratigraphically oldest unit in the map area. The deformation patterns in densely lineated plains material are very dense (spacing is less than 1 km and down to the resolution limit of the Magellan images, about 75 m/px) and unidirectional, and the role of extension in the formation of structural pattern of unit pdl is evident. Although occurrences of the plains are heavily deformed by secondary structures, the overall flatness of the surface suggests that the precursor material was of volcanic origin. Densely lineated plains material makes up a small percentage of the surface outcrop (about 0.9 percent, table 3) and occurs as locally elevated areas in the western and eastern parts of the quadrangle within both the upland of Lada Terra and the surrounding lowlands. Such a distribution suggests a more extensive presence of the unit in the subsurface regardless of the present regional topographic configuration of territory within the quadrangle.

A less deformed plains unit (ridged and grooved plains material, unit prg) was emplaced either contemporaneously or, in part, following the formation of densely lineated plains material. Although little evidence exists for sources, the smooth surface texture of the background material of the unit strongly suggests that it is of volcanic origin. The most important features of ridged and grooved plains are ridges, usually curvilinear structures 5–10 km wide that are very pervasive. The ridges are comparable to contractional structures of the lunar mare. Occurrences of the unit apparently make up a zone of broad arches (from 75–200 km across) running generally in the southwest direction within the lowlands and roughly parallel to the edge of the Lada Terra upland. In the northeast corner of the map area, small and elongated occurrences of the ridged and grooved plains deformed by the ridges are on the northwestern and northern flanks of Lada Terra.

The parallelism of the strike of the tectonic structures (ridges) and broad arches of this unit suggest the same principal strain orientation during formation of both types of features. Thus, the period during which this unit was formed was characterized by emplacement of widespread volcanic plains and their subsequent deformation into broad arches with distinctive ridges by compression forces. Grooves that occasionally complicate fragments of ridge belts indicate late and localized episodes of extension that may be linked to the formation of the arches. Unit prg and its deformation appear to have produced the second-order topography within extensive lowlands in the northern and western parts of the Mylitta Fluctus quadrangle as well as segmentation of the lowlands into secondary small-scale basins by linear and curvilinear arches standing several hundred meters above the surrounding terrain.

After emplacement and deformation of ridged and grooved plains material, another distinctly different plains unit (shield plains material, unit psh) was emplaced in many parts of the map area. Presently exposed occurrences of the unit are seen preferentially in the western and northern parts of the map area around Morrigan Linea and Penardun Linea and as patches in relatively high, but local, areas elsewhere in the quadrangle.

Clusters of small shields characterizing the unit have slightly different radar albedo than surrounding regional plains and typically are outlined by clear sinuous contacts that outline individual shields at the boundaries of the clusters (see also Aubele, 1994). There is no evidence for flows emanating from the shields and superposed on the surface of surrounding regional plains. The density of shields is sharply diminished across the cluster boundaries and only a few small isolated edifices are seen between neighboring clusters. All these criteria collectively suggest that the clusters of shields and shield plains material predate emplacement of vast regional wrinkle-ridged plains material.

The abundant shield volcanoes and intershield plains that are characteristic of this unit are noticeably different from the volcanic style of both previous ridged and grooved plains and subsequent plains with wrinkle ridges. The extent of these vents indicates widespread local and shallow magma sources during the emplacement of shield plains. Unit psh embays ridged and grooved plains material. It is a younger unit manifesting a distinctly different style of volcanism that began in the map area after deformation of unit prg into ridges and arches. Small edifices of shield plains are typically embayed by wrinkle-ridged plains material. This embayment strongly suggests that shield plains material predates emplacement of regional plains units.

Close association of the shield plains material with older material units such as densely lineated plains material and especially ridged and grooved plains material that make up local highs suggests that the topographic position of the unit occurrences was an important factor in their present areal distribution (Ivanov and Head, 2001b). This is consistent with broad embayment of this unit by later plains (Kreslavsky and Head, 1999) and on the basis of the outcrop patterns of subsequent units (wrinkle-ridged plains material) unit psh probably underlies a significant part of wrinkle-ridged plains, at least within the lowlands surrounding Lada Terra. The lack of extensive development of contractional features such as arches and ridge belts within the areas of unit psh could imply that regional compression stresses had further waned before emplacement of the unit.

Subsequent to the emplacement of shield plains material, the style of volcanism changed again (Head and others, 1996). Instead of abundant small shield volcanoes, broad units of plains, now regionally deformed by wrinkle ridges (units pwr_1 and pwr_2), were emplaced from sources that are now rarely visible. The wide extent of these units, especially of the lower unit (unit pwr_1), and the presence on their surface of narrow sinuous channels within the quadrangle and elsewhere (Baker and others, 1992, 1997; Komatsu and Baker, 1994; Basilevsky and Head, 1996) suggest a high-effusion-rate mode of emplacement from a few sources. Such a volcanic style during the formation of wrinkle-ridged plains material is in distinct contrast to the widespread and abundant small shield volcanoes just preceding this phase. Although widespread, wrinkle-ridged plains material appears to be relatively thin (Ivanov and Head, 2001b) because small and large outliers of older units commonly occur within the broad fields of regional plains material (Kreslavsky and Head, 1999).

On the basis of the outcrop distribution of the upper unit of wrinkle-ridged plains material (unit pwr_2), it appears that the sources of this unit may have been distributed in different parts of the map area. These sources may have fed individual deposits in smaller secondary basins that complicate the broad lowlands surrounding the upland of Lada Terra. The largest occurrence of the unit pwr_2 is on the western regional slope of Lada Terra where it is in contact and partly underlies later lobate flows emanating from the Quetzalpetlatl Corona area. These relationships suggest that this occurrence of the upper unit of wrinkle ridged plains may represent early stages of volcanic activity at Quetzalpetlatl Corona.

Materials of wrinkle ridged plains (units pwr_1 and pwr_2) cover about 36 percent of the map area (table 3) and are concentrated predominantly in the lowland areas surrounding Lada Terra between outcrops of belts of ridged and grooved plains and shield plains material. Within the upland of Lada Terra, the wrinkle ridged plains material is almost completely flooded by later lobate plains material and seen within a few stratigraphic windows near Quetzalpetlatl.

The volcanic plains of units pwr_1 and pwr_2 as well as previous shield plains material (unit psh), were further deformed by structures of wrinkle ridges during and subsequent to their emplacement. Some wrinkle ridges in the western part of the map area are oriented generally consistently with the tectonic fabric typical of ridged and grooved plains and approximately circumferential to Lada Terra. Thus, the deformation recorded in units prg, pwr_1 and pwr_2 appears to be consistent in structural trends but reflects decreasing amount of shortening and deformation with time.

The Mylitta Fluctus quadrangle displays a rich geological record of relatively late (post wrinkle-ridged plains material) volcanic and tectonic activity. Small and medium-sized (250–300 km across) and abundant occurrences of smooth plains material (unit ps) are concentrated in the western half of the map area and in its northeastern corner. Some patches of smooth plains in the northwestern part of the quadrangle are in close spatial association with the large impact crater Meitner (table 2). This association suggests that in some places smooth plains material may be related to the impact event and represents fine-grained and morphologically smooth (hence, dark) mantling material ejected by the Meitner event. In many other places, however, smooth plains material has no visible association with impact craters and tends to occur near distinct volcanic centers (for instance, Tarbell Patera), which indicates that areas of smooth plains material at these localities are morphologically smooth and homogeneous facies of late volcanism in the map area.

Lobate and digitate flows that make up units pl_1 and pl_2 were emplaced mostly after formation of wrinkle ridged plains material. Lobate plains material shows clear association with two large volcanic centers that are within the upland of Lada Terra: Jord Corona/Tarbell Patera complex at the northern edge of the upland and Quetzalpetlatl Corona/Boala Corona complex in the west-central part of the upland.

Lobate plains material was apparently emplaced during two major episodes of volcanism. The earlier episode that

produced the lower unit of lobate plains material (unit pl_1) centered at the Jord/Tarbell complex was at least partly contemporaneous with development of the rift zone of Kalaipahoa Linea. The second episode of late volcanism has two apparent sources, Tarbell Patera in the north and Boala Corona, which is completely inside Quetzalpetlatl Corona, in the south. This stage of volcanism has led to formation of enormous lava complexes such as Mylitta Fluctus to the north of Tarbell and Cavillaca and Jatuma Fluctuses southwest of Quetzalpetlatl. These huge lava complexes are characterized by numerous sinuous and overlapping lava flows and have a large extent (about 1,000 km in the case of Mylitta Fluctus, Roberts and others, 1992). There are, however, no large or medium-sized volcanoes associated with the source regions of the fluctuses (Crumpler and Aubele, 2000). This lack of associated volcanoes suggests that although the eruptions that produced these lava complexes were voluminous and at high effusion rate, they probably were not persistent enough to form prominent volcanic edifices.

There is no evidence for the deformation of either smooth plains material or lobate plains material by wrinkle ridges, which suggests that the materials of the plains are very recent and as yet undeformed or that wrinkle ridge deformation as a general phenomenon ceased by this time. Given the decrease in the contractional tectonic deformation intensity as a function of time, the absence of wrinkle ridges in materials of smooth and lobate plains probably resulted from waning deformational forces. In summary, volcanism at the time of formation of smooth plains and lobate plains materials played a significant role in resurfacing and continued to operate as an important factor in formation of the extensive floodlike plains units. This volcanic activity was, however, almost completely restricted within the upland of Lada Terra and related to two major sources in the northern and central parts of the upland.

One of these sources is Quetzalpetlatl Corona, the evolution of which apparently spans a large part of the geologic history of the map area. The oldest materials seen in the corona region and clearly related to its development are deformed into a ridge belt that makes up the northern corona rim and is morphologically akin to the ridge belts elsewhere in the quadrangle. The deformation in the Quetzalpetlatl ridge belt predates emplacement of regional wrinkle ridged plains material (unit pwr_1) meaning that the corona was in its place relatively early on in the geologic history of the quadrangle. The young (post regional plains) and voluminous volcanism related to Quetzalpetlatl unequivocally implies that the corona was active until the latest documented episodes of the geologic history. Topographically, Quetzalpetlatl represents a large dome-shaped highland topped with a caldera-like Boala Corona (fig. 2, Ivanov and Head, 2003). These characteristics of the corona are consistent with an interpretation of the late broad updoming that was centered over Quetzalpetlatl. The heavy flooding of the area by young lava flows prevents detailed documentation of the sequence of events at the corona. Consequently, both explanations of its evolution as either continuous or discrete (for instance, late reactivation) are plausible. However, the tectonic activity at Quetzalpetlatl was relatively minor and restricted to early epochs of the geologic history within the quadrangle. In sharp contrast, Artemis Corona is characterized by relatively minor volcanism and very rich tectonism that apparently accompanied the whole evolution of Artemis (Brown and Grimm, 1995, 1999; Spenser, 2001; Hansen, 2002; Ivanov and Head, 2003).

Of the nine impact craters in the map area (fig. 4, table 2), eight are within the lowlands surrounding Lada Terra upland where the craters are superimposed on the surface of regional wrinkle-ridged plains material (units pwr_1 and pwr_2) and, therefore, postdate the plains units. One of the craters, Alcott (table 2), is southeast of Tarbell Patera (fig. 4) and heavily embayed by volcanic flows of the upper unit of lobate plains material (unit pl_2, fig. 13) but it is superimposed on the surface of lower unit of lobate plains material (unit pl_1). Within the map area, no craters were possibly cut by tectonic structures. Because no craters embayed by pre-lobate plains units were observed and because the widespread deposits of wrinkle-ridged plains material are considered relatively thin, we think the lack of embayed craters indicates that the plains units were probably emplaced in a relatively short period of geologic time. This interpretation is, however, tentative owing to the small total number of craters (Campbell, 1999).

The embayed crater, Alcott, is 66 km in diameter (table 2). The interior of the crater is completely flooded and there is no evidence for a central structure, but the crater rim is clearly visible and continues for about 70 percent of the total rim length. The data on morphometry of Venusian craters (Sharpton, 1994; Herrick and Sharpton, 2000) indicate that for a 70-km-diameter crater the height of the central structure could be as much as 200 m. This value, therefore, is the minimum estimate of the thickness of flooding plains within the crater Alcott. The height of the rim above the surrounding terrain for a crater of the size of Alcott is about 0.3–0.4 km (Herrick and Sharpton, 2000). That almost the entire rim of Alcott stands above the surrounding plains, except for the breached part, means the thickness of the plains in close proximity to the crater should be significantly less than the rim height and suggests that maximum thickness of lobate plains there is less than a few hundred meters.

There are clear trends in the evolution of tectonic regimes within the Mylitta Fluctus quadrangle. Contractional deformation changed from that associated with the formation of compact ridge belts deforming ridged and grooved plains material (unit prg, figs. 6, 7) to that associated with deformation of regional wrinkle-ridged plains material (units pwr_1 and pwr_2) by pervasive structures of wrinkle ridges (figs. 8, 9). Contractional structures are absent within younger plains units such as smooth and lobate plains materials (units ps, pl_1, and pl_2, figs. 9–12); this lack of contractional structures suggests cessation of compression stresses by the time these units were emplaced.

Extensional deformation that overprints densely lineated plains material (unit pdl) and played a major role in the formation of groove belts (unit gb) and rift zones (unit rt) appears to have an opposite trend. Fractures that have shaped the surface of material unit pdl are very narrow, pervasive, and do not form beltlike concentrations. The subsequent occurrences of

extensional structures are organized into belts, of which many structures become progressively broader as a function of time. However, some occurrences of groove belts concentrated in the northwestern corner of the map area continue the general trend of the Kalaipahoa Linea rift zone. This contrasting pattern suggests that the rift, as a younger zone of deformation, probably inherited the structural trend of older groove belts and may have resulted from reactivation of a precursor deformation belt. Thus, the general orientation of tensional stresses appears to be stable through a significant part of geologic history within the quadrangle, from before the emplacement of regional wrinkle-ridged plains material (unit pwr_1) to the time of formation of lobate plains material (unit pl_1). Except for a few graben outlining the rim of Boala Corona, the upper unit of lobate plains material (unit pl_2) is tectonically undeformed. This means that either any regional tectonic activity ceased by the time of emplacement of this unit or it is very young and has not yet been deformed.

The graben radiating away from the Jord Corona, as well as Nike and Enyo Fossae, are apparently related to a local stress regime centered at the corona. Three features characterize these graben. (1) Planimetrically, they are straight, narrow, and very long (as much as 400–450 km). (2) Elongated and oval-shaped depressions are often attached to the graben ends near Jord Corona. (3) In places, lava flows appear to be spatially associated with the graben. These characteristics suggest that the graben represent the surface manifestation of dikes (Grosfils and Head, 1994, 1996; Ernst and others, 2001; Krassilnikov and Head, 2003) propagating from the topographically higher volcanic center of Jord Corona.

The large-scale topography of the Mylitta Fluctus quadrangle (fig. 2) shows the transition zone from the upland of Lada Terra to the lowlands, one of which is Lavinia Planitia. The basin of Lavinia is a broad lowland region, the central parts of which are characterized by abundant deformation belts such as ridges and arches (Squyres and others, 1992) of ridged and grooved plains material (unit prg, Ivanov and Head, 2001a). Formation of these belts is consistent with local crustal shortening, thickening, and buckling in response to broad subsidence of the surface of the basin (Squyres and others, 1992). Within the western part of Mylitta Fluctus quadrangle, a prominent zone of arches and ridge belts (Morrigan Linea) runs within the lowlands roughly parallel to the western edge of the Lada Terra upland. In the northeastern corner of the quadrangle, however, arches and ridge belts of Molpadia and Penardun Lineas, which are the southern continuation of the Lavinia Planitia deformational belts, occur at northern and northwestern flanks of the upland. There the belts are heavily embayed by lobate plains material and cut by rift structures of Kalaipahoa Linea. If the arches and belts formed in response to subsidence of the broad Lavinia Planitia basin (Squyres and others, 1992), then their presence within Lada Terra suggests that at least the western part of Lada began to rise after deformation of ridged and grooved plains material (unit prg) into ridge belts. Thus, the time of deformation of the plains is probably the lower stratigraphic limit for the formation of western part of the Lada Terra upland.

Another constraint on the evolution of the western part of Lada Terra is provided by flowlike features that characterize the largest occurrence of the upper unit of wrinkle-ridged plains material (unit pwr_2) in the map area. This field of unit pwr_2 is on western regional slope of Lada Terra and lava flows within it are generally oriented in an east-west direction along the present-day topographic gradient. This distribution of the flows suggests that the western part of Lada Terra topographic province was already elevated by the time of emplacement of material unit pwr_2. Volcanic flows within later lobate plains material (units pl_1 and pl_2) clearly follow the present-day topography meaning that the large-scale topographic characteristics within the map area have not changed since the youngest material units were emplaced.

Acknowledgements: Thanks are extended to Alexander Basilevsky and Jayne Aubele for detailed discussion about regional and global units and relations. We particularly appreciate the helpful discussions that occurred during the annual Planetary Geologic Mappers meetings and during an informal mapping workshop held at Brown University in the summer of 1995 and attended by George McGill, Steve Saunders, Jim Zimbelman, Alexander Basilevsky, Elizabeth Rosenberg, and Nathan Bridges. Their comments and discussions were most helpful in this effort. Constructive reviews of the map by M.S. Gilmore and R. Ghent, and K. Tanaka are deeply appreciated. Financial support from the NASA Planetary Geology and Geophysics Program (Grant NAGW-5023) is gratefully acknowledged.

REFERENCES CITED

Addington, E.A., 2001, A stratigraphic study of small volcano clusters on Venus: Icarus, v. 149, p. 16–36.

Aubele, J.C., 1994, Stratigraphy of small volcanoes and plains terrain in Vellamo Planitia, Venus, *in* Lunar and Planetary Science Conference, 25th, Houston, Texas, March 14–18, 1994, Abstracts, p. 45–46.

Aubele, J.C., 1995, Stratigraphy of small volcanoes and plains terrain in Vellamo Planitia-Shimti tessera region, Venus, *in* Lunar and Planetary Science Conference, 26th, Houston, Texas, March 13–17, 1995, Abstracts, p. 59–60.

Aubele, J.C., and Slyuta, E.N., 1990, Small domes on Venus: Characteristics and origin: Earth, Moon and Planets, v. 50/51, p. 493–532.

Baer, G., Schubert, G., Bindschadler, D.L., and Stofan, E.R., 1994, Spatial and temporal relations between coronae and extensional belts, Northern Lada Terra, Venus: Journal of Geophysical Research, v. 99, p. 8355–8369.

Baker, V.R., Komatsu, Goro, Gulick, V.C., and Parker, T.J., 1997, Channels and valleys, *in* Phillips, R.J., and others, eds., Venus II: Tucson, University of Arizona Press, p. 757–793.

Baker, V.R., Komatsu, Goro, Parker, T.J., Gulick V.C., Kargel, J.S., and Lewis, J.S., 1992, Channels and valleys on Venus: Preliminary analysis of Magellan data: Journal of Geophysical Research, v. 97, p. 13421–13444.

Basilevsky, A.T., and Head, J.W., 1995a, Global stratigraphy

of Venus—Analysis of a random sample of thirty-six test areas: Earth, Moon and Planets, v. 66, p. 285–336.

Basilevsky, A.T., and Head, J.W., 1995b, Regional and global stratigraphy of Venus—A preliminary assessment and implications for the geologic history of Venus: Planetary Space Science, v. 43, p. 1523–1553.

Basilevsky, A.T., and Head, J.W., 1996, Evidence for rapid and widespread emplacement of volcanic plains on Venus: Stratigraphic studies in the Baltis Vallis region: Geophysical Research Letters, v. 23, p. 1497–1500.

Basilevsky, A.T., and Head, J.W., 2002, Venus: Analysis of the degree of impact crater deposit degradation and assessment of its use for dating geologic units and features: Journal of Geophysical Research, v. 107, p. 5-1 to 5-38.

Basilevsky, A.T., Head, J.W., Schaber, G.G., and Strom, R.G., 1997, The resurfacing history of Venus, *in* Phillips, R.J., and others, eds., Venus II: Tucson, University of Arizona Press, p. 1047–1084.

Basilevsky, A.T., Nikolaeva, O.V., and Weitz, C.M., 1992, Geology of the Venera 8 landing site region from Magellan data: Morphological and geochemical considerations: Journal of Geophysical Research, v. 97, p. 16,315–16,335.

Bindschadler, D.L., Decharon, A., Beratan, K.K., Smrekar, S.E., and Head, J.W., 1992a, Magellan observations of Alpha Regio: Implications for formation of complex ridged terrains on Venus: Journal of Geophysical Research, v. 97, p. 13,563–13,578.

Bindschadler, D.L., Schubert, Gerald, and Kaula, W.M., 1992b, Coldspots and hotspots—Global tectonic and mantle dynamics of Venus: Journal of Geophysical Research, v. 97, p. 13,495–13,532.

Bridges, N.T., and McGill, G.E., 2002, Geologic map of the Kaiwan Fluctus quadrangle (V–44), Venus: U.S. Geological Survey Geologic Investigations Series I–2747 [available at http://geopubs.wr.usgs.gov/i-map/i2747/].

Brown, C.D., and Grimm, R.E., 1995, Tectonics of Artemis Chasma: A venusian "plate" boundary: Icarus, v. 117, p. 219–249.

Brown, C.D., and Grimm, R.E., 1999, Recent tectonic and lithospheric thermal evolution of Venus: Icarus, v. 139, p. 40–48.

Campbell, B.A., 1995, Use and presentation of Magellan quantitative data in Venus mapping: U.S. Geological Survey Open File Report 95–519, 32 p.

Campbell, B.A., 1999, Surface formation rates and impact crater densities on Venus: Journal of Geophysical Research, v. 104, p. 21951–21955.

Campbell, B.A., and Campbell, P.G., 2002, Geologic map of the Bell Regio quadrangle (V–9), Venus: U.S. Geological Survey Geologic Investigations Series I–2743 [available at http://geopubs.wr.usgs.gov/i-map/i2743/].

Campbell, D.B., Senske, D.A., Head, J.W., Hine, A.A., and Fisher, P.C., 1991, Venus southern hemisphere—Geologic characteristics and ages of major terrains in the Themis-Alpha-Lada region: Science, v. 251, p. 180–183.

Campbell, D.B., Stacy, N.J.S., Newman, W.I., Arvidson, R.E., Jones, E.M., Musser, G.S., Roper, A.Y., and Schaller, Christian, 1992, Magellan observations of extended crater related features on the surface of Venus: Journal of Geophysical Research, v. 97, p. 16,249–16,277.

Crumpler, L.S., and Aubele, J.C., 2000, Volcanism on Venus, *in* Sigurdsson, Haraldur, ed., Encyclopedia of volcanoes, San Diego, Academic Press, p. 727–770.

Crumpler, L.S., Head, J.W., and Aubele, J.C., 1993, Relation of major volcanic center concentration on Venus to global tectonic patterns: Science, v. 261, p. 591–595.

Elachi, Charles, 1987, Introduction to the physics and techniques of remote sensing: New York, Wiley and Sons, 413 p.

Ernst, R.E., Grosfils, E.B., and Mege, D., 2001, Giant dike swarms—Earth, Venus, and Mars: Annual Review Earth Planet, Science, v. 29, p. 489–534.

Ford, P.G., and Pettengill, G.H., 1992, Venus topography and kilometer-scale slopes: Journal of Geophysical Research, v. 97, p. 13,102–13,114.

Ford, P.G., Plaut, J.J., Weitz, C.M., Farr, T.G., Senske, D.A., Stofan, E.R., Michaels, Gregory., and Parker, T.J., eds., 1993, Guide to Magellan image interpretation: Pasadena, Calif., Jet Propulsion Laboratory Publication 93–24, 148 p.

Frank, S.L., and Head, J.W., 1990, Ridge Belts on Venus—Morphology and Origin: Earth, Moon, and Planets, v. 50/51, p. 421–470.

Greeley, Ronald, Arvidson, R.E., Elachi, Charles, Geringer, M.A., Plaut, J.J., Saunders, R.S., Schubert, Gerald, Stofan, E.R., Thouvenot, E.J.P., Wall, S.D., and Weitz, C.M., 1992, Aeolian features on Venus—Preliminary Magellan results: Journal of Geophysical Research, v. 97, p. 13,319–13,345.

Greeley, Ronald, and Guest, J.E., 1987, Geologic map of the eastern equatorial region of Mars: U.S. Geological Survey Miscellaneous Investigations Series Map I–1802–B, scale 1:15,000,000.

Grosfils, E.B., and Head, J.W., 1994, The global distribution of giant radiating dike swarms on Venus—Implications for the global stress stare: Geophysical Research Letters, v. 21, p. 701–704.

Grosfils, E.B., and Head, J.W., 1996, The timing of giant radiating dike swarm emplacement on Venus—Implications for resurfacing of the planet and its subsequent evolution: Journal of Geophysical Research, v. 101, p. 4645–4656.

Guest, J.E., Bulmer, M.H., Aubele, J.C., Beratan, K.K., Greeley, Ronald, Head, J.W., Michaels, G.A., Weitz, C.M., and Wiles, C.R., 1992, Small volcanic edifices and volcanism in the plains of Venus: Journal of Geophysical Research, v. 97, p. 15,949–15,966.

Hansen, V.L., 2002, Artemis: Surface expression of a deep mantle plume on Venus: Geological Society of America, Bulletin, v. 114, p. 839–848.

Hansen, V.L., and DeShon, H.R., 2002, Geologic map of the Diana Chasma quadrangle (V–9), Venus: U.S. Geological Survey Geologic Investigations Series I-2752 [available at http://geopubs.wr.usgs.gov/i-map/i2752/].

Hansen, V.L., Willis, J.J., and Banerdt, W.B., 1997, Tectonic overview and synthesis, *in* Phillips, R.J., and others, eds., Venus II: Tucson, University of Arizona Press, p. 797–844.

Hauck, S.A., Phillips, R.J., and Price, M.H., 1998, Venus: Crater distribution and plains resurfacing models: Journal of Geophysical Research, v.103, p. 13635–13642.

Head, J.W., Basilevsky, A.T., Wilson, Lionel, and Hess, P.C., 1996, Evolution of volcanic styles on Venus: Change, but not Noachian? [abs.]: Lunar and Planetary Science Conference, 27th, Houston, Texas, March 13–17, 1996, Abstracts, p. 525–526.

Head, J.W., Crumpler, L.S., Aubele, J.C., Guest, J.E., and Saunders, R.S., 1992, Venus volcanism—Classification of volcanic features and structures, associations, and global distribution from Magellan data: Journal of Geophysical Research, v. 97, p. 13153–13197.

Herrick, R.R., and Sharpton, V.L., 2000, Implications from stereo-derived topography of Venusian impact craters: Journal of Geophysical Research, v. 105, p. 20245–20262.

Herrick, R.R., Sharpton, V.L., Malin, M.C., Lyons, S.N., and Feely, K., 1997, Morphology and morphometry of impact craters, *in* Phillips, R.J., and others, eds., Venus II: Tucson, University of Arizona Press, p. 1015–1046.

Ivanov, B.A., Nemchinov, I.V., Svetsov, V.A., Provalov, A.A., Khazins, V.M., and Phillips, R.J., 1992, Impact cratering on Venus: Physical and mechanical models: Journal of Geophysical Research, v. 92, p. 16,167–16,181.

Ivanov, M.A., and Basilevsky, A.T., 1993, Density and morphology of impact craters of tessera terrain, Venus: Geophysical Research Letters, v. 20, p. 2579–2582.

Ivanov, M.A., and Head, J.W., 1996, Tessera terrain on Venus: A survey of the global distribution, characteristics, and relation to surrounding units: Journal of Geophysical Research, v. 101, p. 14,861–14,908.

Ivanov, M.A., and Head, J.W., 1998, Major issues in Venus geology: Insights from a global geotraverse at 30N latitude: Lunar and Planetary Science Conference, 29th, Houston, Texas, March 16–20, 1998, Abstract 1419.

Ivanov, M.A., and Head, J.W., 2001a, Geologic map of the Lavinia Planitia (V55) quadrangle: U.S. Geological Survey Geologic Investigations Series I–2684, scale 1:5,000,000 [available at http://geopubs.wr.usgs.gov/i-map/i2684/].

Ivanov, M.A., and Head, J.W., 2001b, Geology of Venus: Mapping of a global geotraverse at 30° N. latitude: Journal of Geophysical Research, v. 106, p. 17515–17566.

Ivanov, M.A., and Head, J.W., 2003, Evolution of three largest coronae on Venus, Heng-O, Quetzalpetlatl, and Artemis: Preliminary results, *in* Lunar and Planetary Science Conference XXXIV, abstract 1188 [CD-ROM].

Kiefer, W.S., and Hager, B.H., 1991, A mantle plume model for the equatorial highlands of Venus: Journal of Geophysical Research, v. 96, 20947–20966.

Komatsu, Goro, and Baker, V.R., 1994, Longitudinal profiles of plains channels on Venus: Lunar and Planetary Science Conference, 25th, Houston, Texas, March 16–20, 1994, p. 727–728.

Konopliv, A.S., Banerdt, W.B., and Sjogren, W.L., 1999, Venus gravity: 180th degree and order model: Icarus, v. 139, p. 3–18.

Konopliv, A.S., and Sjogren, W.L., 1994, Venus spherical harmonic gravity model to degree and order 60: Icarus, v. 112, p. 42–54.

Krassilnikov, A.S., and Head, J.W., 2003, Novae on Venus: Geology, classification and evolution: Journal of Geophysical Research, v. 108, no. E9.

Kreslavsky, M.A., and Head, J.W., 1999, Morphometry of small shield volcanoes on Venus—Implications for the thickness of regional plains: Journal of Geophysical Research, v. 104, p. 18925–18932.

Kryuchkov, V.P., 1990, Ridge Belts: Are They Compressional or Extensional Structures?: Earth, Moon, and Planets, v. 50/51, p. 471–491.

Magee, K.P., and Head, J.W., 1995, The role of rifting in the generation of melt—Implications for the origin and evolution of the Lada Terra-Lavinia Planitia region on Venus: Journal of Geophysical Research, v. 100, p. 1527–1552.

Masursky, Harold, Eliason, Eric, Ford, P.G., McGill, G.E., Pettengill, G.H., Schaber, G.G., and Schubert, Gerald, 1980, Pioneer-Venus radar results: geology from the images and altimetry: Journal of Geophysical Research, v. 85, p. 8232-8260.

McKinnon, W.B., Zahnle, K.J., Ivanov, B.A., and Melosh, H.J., 1997, Cratering on Venus: Models and observations, *in* Phillips, R.J., and others, eds., Venus II: Tucson, University of Arizona Press, p. 969–1014.

Mescherikov, Y.A., 1968, Plains, *in* Fairbridge, R.W., ed., Encyclopedia of Geomorphology: New York, Reinhold Book Corporation, 1295 p.

North American Commission on Stratigraphic Nomenclature, 1983, Code of Stratigraphic Nomenclature: American Association of Petroleum Geologists Bulletin, v. 67, no.5, p. 841–875.

Pavri, Betina, Head, J.W., Klose, K.B., and Wilson, Lionel, 1992, Steep-sided domes on Venus: Characteristics, geologic setting, and eruption conditions from Magellan data: Journal of Geophysical Research, v. 97, p. 13,445–13,478.

Pettengill, G.H., Eliason, Eric, Ford, P.G., Loriot, G.B., Masursky, Harold, and McGill, G.E., 1980, Pioneer Venus radar results—Altimetry and surface properties: Journal of Geophysical Research, v. 85, p. 8261–8270.

Phillips, R.J., Raubertas, R.F., Arvidson, R.E., Sarkar, E.C., Herrick, R.R., Izenberg, Noam, and Grimm, R.E., 1992, Impact craters and Venus resurfacing history: Journal of Geophysical Research, v. 97, p. 15,923–15,948.

Phillips, R.J., and Hansen, V.L., 1998, Geological evolution of Venus—Rises, plains, plumes, and plateaus: Science, v. 279, p. 1492–1497.

Roberts, K.M., Guest, J.E., Head, J.W., and Lancaster, M.G., 1992, Mylitta Fluctus, Venus—Rift-related, centralized volcanism and the emplacement of large-volume flow units: Journal of Geophysical Research, v. 97, p.15991–16016.

Rosenberg, Elizabeth, and McGill, G. E., 2001, Geologic map of the Pandrosos Dorsa quadrangle (V–5), Venus: U.S. Geological Survey Geologic Investigations Series I–2721 [available at http://geopubs.wr.usgs.gov/i-map/i2721/].

Saunders, R.S., and 26 others, 1992, Magellan mission summary: Journal of Geophysical Research, v. 97, p. 13,067–13,090.

Schaber, G.G., Strom, R.G., Moore, H.J., Soderblom, L.A., Kirk, R.L., Chadwick, D.J., Dawson, D.D., Gaddis, L.R., Boyce, J.M., and Russell, Joel, 1992, Geology and distribution of impact craters on Venus—What are they telling us?: Journal of Geophysical Research, v. 97, p. 13,257–13,302.

Schaber, G.G., Kirk, R.L., and Strom, R.G., 1998, Data Base of Impact Craters on Venus Based On Analysis of Magellan Radar Images and Altimetry Data : U.S. Geological Survey Open-File Report 98–104.

Schultz, P.H., 1992, Atmospheric effects on ejecta emplacement and crater formation on Venus from Magellan: Journal of Geophysical Research, v. 97, p. 183–248.

Scott, D.H., and Tanaka, K.L., 1986, Geologic map of the western equatorial region of Mars: U.S. Geological Survey Miscellaneous Investigations Series Map I–1802–A, scale 1:15,000,000.

Senske, D.A., Campbell D.B., Head, J.W., Fisher, P., Hine, A., deCharon, A., Frank, S., Keddie, S., Roberts, K., Stofan, E.R., Aubele, J.C., Crumpler, L.S., and Stacy, N., 1991, Geology and tectonics of the Themis Regio–Lavinia Planita–Alpha Regio–Lada Terra area, Venus—Results from Arecibo image data: Earth, Moon, and Planets, v. 55, p. 97–161.

Sharpton, V.L., 1994, Evidence from Magellan for unexpectedly deep complex craters on Venus, *in* Dressler, B.O., Grieve, R.A.F., and Sharpton, V.L., eds., Large meteorite impacts and planetary evolution: Geological Society of America Special Paper 293, p. 19–27.

Solomon, S.C., Smrekar, S.E., Bindschadler, D.L., Grimm, R.E., Kaula, W.M., McGill, G.E., Phillips, R.J., Saunders, R.S., Schubert, Gerald, Squyres, S.W., and Stofan, E.R., 1992, Venus tectonics—An overview of Magellan observations: Journal of Geophysical Research, v. 97, p. 13,199–13,256.

Spenser, J.E., 2001, Possible giant metamorphic core complex at the center of Artemis Corona, Venus: Geological Society of America, Bulletin, .v. 113, p. 333–345.

Squyres, S.W., Jankowski, D.G., Simons, Mark, Solomon, S.C., Hager, B.H., and McGill, G.E., 1992, Plains tectonism on Venus—The deformation belts of Atalanta Planitia: Journal of Geophysical Research, v. 97, p. 13,579–13,600.

Stofan, E.R., Sharpton, V.L., Schubert, Gerald, Baer, Gidon, Bindschadler, D.L., Janes, D.M., and Squyres, S.W., 1992, Global distribution and characteristics of coronae and related features on Venus—Implications for origin and relation to mantle processes: Journal of Geophysical Research, v. 97, p. 13347–13378.

Stofan, E.R., Smrekar, S.E., Tapper, S.W., Guest, J.E., and Grindrod, P.M., 2001, Preliminary analysis of an expanded corona database for Venus: Geophysical Research Letters, v. 28, p. 4267–4270.

Strom, R.G., Schaber, G.G., and Dawson, D.D., 1994, The global resurfacing of Venus: Journal of Geophysical Research, v. 99, p. 10,899–10,926.

Tanaka, K.L., 1994, Venus geologic mappers' handbook, 2nd ed.: U.S. Geological Survey Open-File Report 94–438, 68 p.

Tyler, G.L., Simpson, R.A., Maurer, M.J., and Holmann, Edgar, 1992, Scattering properties of the venusian surface—Preliminary results from Magellan: Journal of Geophysical Research, v. 97, p. 13,115–13,140.

Wilhelms, D.E., 1990, Geologic mapping, *in* Greeley, Ronald, and Batson R.M., eds., Planetary mapping: New York, Cambridge University Press, p. 208–260.

Table 1. *List of volcanic and volcano-tectonic features in the Mylitta Fluctus quadrangle (modified from Crumpler and Aubele, 2000)*

Latitude	Longitude	Diameter, km	Feature name
		Large Volcanoes	
–58.5	351	~100	—
		Intermediate Volcanoes 1: Fluted or Modified Domes	
–61.5	331	20	—
–62	328.5	60	—
–63.5	325.5	20	—
–63.5	327.5	20	—
		Intermediate Volcanoes 2: Steep-sided domes	
–50.7	305.9	31	—
–51.1	305.6	34	—
–51.2	305.5	48	—
–51.4	305.3	470	—
		Paterae	
–53	352.5	220	Tarbell
		Coronae	
–50.5	301	100	—
–70	306	250	—
–50.5	306.5	80	—
–63.5	322	300	Kamui-Huci Corona
–59	350	220	Jord Corona
–68	355	>700	Quetzalpetlatl Corona

[—, no official name has been assigned to this feature.]

Table 2. *List of impact craters within the Mylitta Fluctus quadrangle (modified from Schaber and others, 1998).*

Crater Name	Latitude	Longitude	Diameter, km	Elevation, km
Mildred	–51.7	348.3	12.0	0.10
Grey	–52.4	329.4	50.0	0.20
Nadeyka	–54.8	305.3	9.3	0.61
Meitner	–55.6	321.6	149.0	0.64
Alcott	–59.52	354.4	66.0	1.27
Jane	–60.5	304.8	10.2	0.63
Kristina	–65.2	315.9	9.7	0.48
Sandi	–68.1	315.1	12.6	-0.01
Melina	–69.9	319.5	12.7	-0.23

Table 3. *Area of units mapped in the Mylitta Fluctus quadrangle.*

Unit	area, km^2	area, %
pdl	70,910	0.9
prg	413,562	5.4
gb	92,908	1.2
psh	644,432	8.4
pwr_1	2,079,365	27.1
pwr_2	673,081	8.8
ps	544,501	7.1
pl_1	902,068	11.8
pl_2	1,177,801	15.4
sc	3,886	0.1
rt	261,814	3.4
c	61,383	0.8
no data	738,284	9.6
TOTAL	7,663,996	100